Indian Journal of Pure & Applied Physics
Vol. 61, September 2023, pp. 723-726
DOI: 10.56042/ijpap.v61i9.3406

Structural and Optical Properties of α-Fe_2O_3/ZnO Nanocomposite in Wastewater Treatment

Sonia[a], Harita Kumari[b], Monica[a], Sourabh Sharma[c], Seema Devi[c], Surjeet Chahal[d], Suman[a], Parmod Kumar[e*] & Ashok Kumar[a*]

[a]Deenbandhu Chhotu Ram University of Science and Technology, Murthal, Haryana 131039, India

[b]Department of Physics, Maharshi Dayanand University, Rohtak, Haryana 124 001, India

[c]Department of Physics, Netaji Subhas University of Technology, Dwarka, New Delhi 110 078, India

[d]Materials and Nano Engineering Research Laboratory, Department of Physics, School of Physical Sciences, DIT University, Dehradun 248 009, India

[e]Department of Physics, J.C.Bose University of Science and Technology, YMCA, Faridabad, Haryana 121 006, India

Received 7 July 2023; accepted 10 August 2023

This study aims to investigate the structural and optical characteristics of pure α-Fe_2O_3, ZnO, and α-Fe_2O_3/ZnO nanocomposite synthesized by hydrothermal method and their application in the purification of dye-contaminated water. Synthesized samples were characterized by XRD, UV, and FTIR. XRD pattern of α-Fe_2O_3/ZnO nanocomposite revealed two distinct phases corresponding to α-Fe_2O_3 and ZnO in synthesized nanocomposite. The characteristic absorbance peaks of α-Fe_2O_3/ZnO nanocomposite were observed in UV visible spectra with a bandgap of 2.50 eV. The photocatalytic properties of as-synthesized nanocomposite have been evaluated by photodegradation of methylene blue (MB) under UV irradiation. Compared to pure metal oxides (α-Fe_2O_3 and ZnO), photodegradation efficiency of nanocomposite for methylene blue dye was found to be enhanced. *i.e.*, 78% in 105 minutes. This improved photocatalytic activity can be ascribed to efficient charge transfer in the nanocomposite, which in turn can be attributed to the reduced recombination probability of photo-induced carriers. The as-synthesized nanocomposite could be appropriate for wastewater treatment dye.

Keywords: Wastewater Treatment; α-Fe_2O_3/ZnO; Photodegradation; Methylene blue dye

1 Introduction

Tremendous increases in industries may have catastrophic consequences for both marine life and humans. Synthetic dyes, which are regularly discharged from industries, are the major reason for water pollution. A significant source of dye pollution is the textile industry. About 10–15% of dyes are discharged directly into aquatic ecosystems without proper treatment. Photocatalysis has been proven to be the most preferable procedure for wastewater treatment due to its cost-effectiveness, and low energy consumption. Numerous substances have been used for degradation of dye-contaminated water, including ZnO, TiO_2, CeO_2, α–Fe_2O_3, SnO_2, MgO, Cu_2O, ZrO_2[1,2]. Among these, hematite (α–Fe_2O_3) is a common semiconductor used as a catalyst for dye degradation because of its abundance, affordability, and environmental friendliness. Despite these characteristics, α-Fe_2O_3 has a high recombination rate due to limited diffusion pathways (2-4 nm) and weak oxidation capacities of holes. Therefore, more active material with a large surface area must be introduced into the host matrix. Many scientists put their endeavours to improve photocatalytic activity by synthesizing nanocomposites such as α–Fe_2O_3@TiO_2, α–Fe_2O_3@ZnO, α–Fe_2O_3@SnO_2, ZnO@ZnS[3-6]. To get rid of surface imperfections, a protective layer could be formed on the surface of nanoparticles which improved the photostability of material by decreasing dangling bond. Herein, we have prepared pure α-Fe_2O_3, pure ZnO, and α–Fe_2O_3/ZnO nanocomposite by cost-effective hydrothermal route for degradation of MB dye.

2. Preparation of α–Fe_2O_3/ZnO Nanocomposite

The hydrothermal technique was utilised to synthesize nanocomposite of α–Fe_2O_3 and ZnO. Firstly, pure α–Fe_2O_3 was synthesized by taking $Fe(NO_3)_2.6H_2O$ and $CO(NH_2)_2$ as precursors. Then 6 mmol of $Zn(NO_3)_2.6H_2O$ and 9 mmol of $CO(NH_2)_2$ were dissolved in 60 ml of distilled water under

*Corresponding authors: (E-mail: ashokkumar.phy@dcrustm.org; kumarparmod@jcboseust.ac.in)

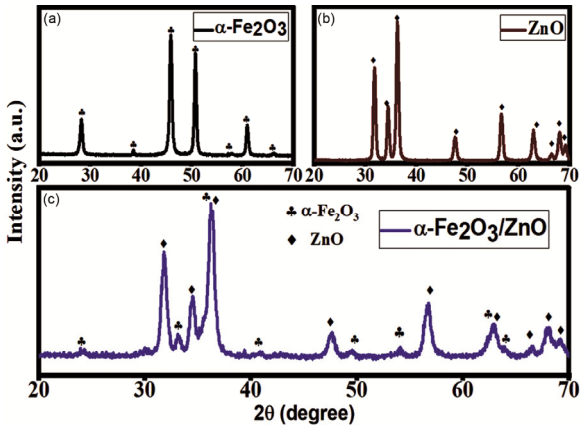

Fig. 1 — XRD pattern of (a) pure α–Fe_2O_3 (b) pure ZnO and (c) α–Fe_2O_3/ZnO nanocomposite.

Table 1 — Structural and UV- Visible spectroscopic results

Samples	Crystallite size (D)nm	Band gap (eV)	% degradation
α–Fe_2O_3	29.10	2.22	50
ZnO	15.45	3.06	43
α–Fe_2O_3/ZnO	11.77	2.50	78

constant stirring. The same solution was then supplemented with the precise quantity of pure α-Fe_2O_3. The resultant mixture was put into a 100 ml Teflon-Lined stainless-steel autoclave, where it experienced hydrothermal treatment at 120 °C for 8 hours. Then resultant precipitates were collected and dried at 80 °C for 20 hours after being repeatedly cleaned with distilled water and ethanol. These samples were then annealed at 500 °C for 2 hours to obtain the α-Fe_2O_3 and ZnO nanocomposites.

3. Results and Discussions

3.1. X-Ray Diffraction

Figure 1 shows XRD pattern of synthesized samples. The crystallite size was calculated using Debye Scherer's formula for pure α-Fe_2O_3, ZnO and α–Fe_2O_3/ZnO nanocomposite as shown in Table 1. Diffracted peaks of α-Fe_2O_3 showed rhombohedral structures which were consistent with the JCPDS card no. (84–0311)[7]. The calculated lattice parameters for α–Fe_2O_3 were found to be *a*–axis = 5.019 Å and *c*–axis = 13.687 Å. The diffraction peaks of ZnO showed a hexagonal structure (JCPDS card no 01-1136)[8]. The calculated lattice parameter for ZnO was found to be *a*–axis = 3.246 Å and *c*–axis=5.175 Å. The synthesized nanocomposite comprised all the peaks as depicted in pure α–Fe_2O_3 and pure ZnO. No other diffraction peaks were observed which indicate high phase purity of synthesized nanocomposite.

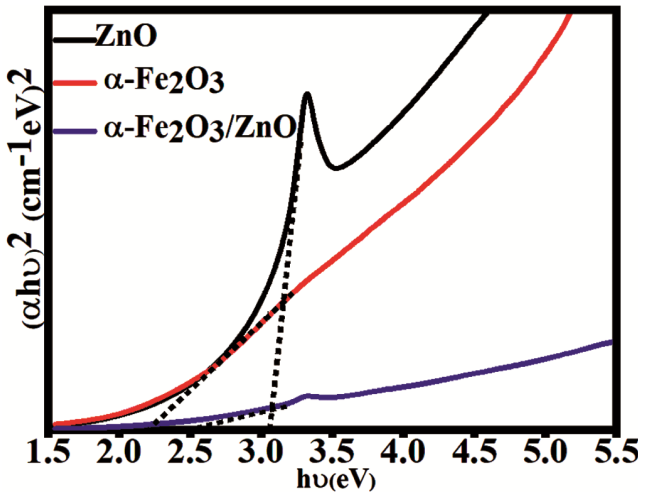

Fig. 2 — Tauc's plot of pure α-Fe_2O_3, pure ZnO and α-Fe_2O_3/ZnO nanocomposite.

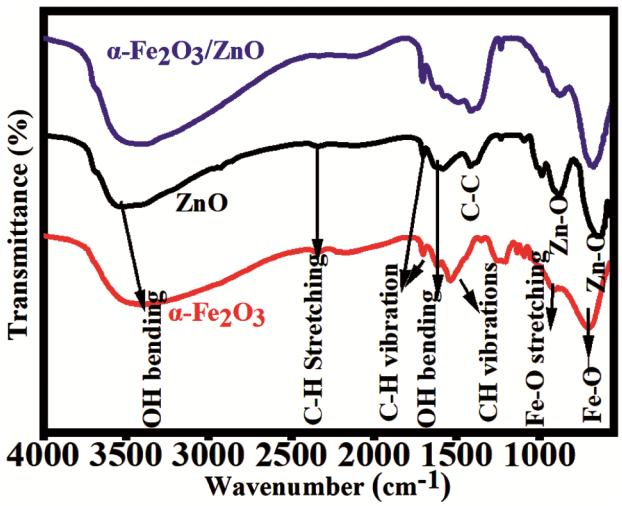

Fig. 3 — FTIR spectra of pure α–Fe_2O_3, pure ZnO and α-Fe_2O_3/ZnO nanocomposite.

3.2. UV-Vis spectroscopy

Figure 2 shows Tauc's plot between $(\alpha h\nu)^{1/2}$ versus (hν) which determines the optical bandgap of pure α–Fe_2O_3, pure ZnO and α–Fe_2O_3/ZnO nanocomposite by employing UV–Vis spectroscopy. The optical band gap values for synthesized samples are depicted in Table 1.The reason for change in band gap was the synergic effect between α–Fe_2O_3 and ZnO.

3.3. FTIR analysis

Fig. 3 shows FTIR spectra of aforementioned synthesized samples in the range of 400-4000 cm^{-1} wave number which identified the chemical bonds/functional groups. The large broadband at 3416 cm^{-1}, and 3476 cm^{-1} is ascribed to O-H stretching vibration of hydroxyl group in α–Fe_2O_3 and

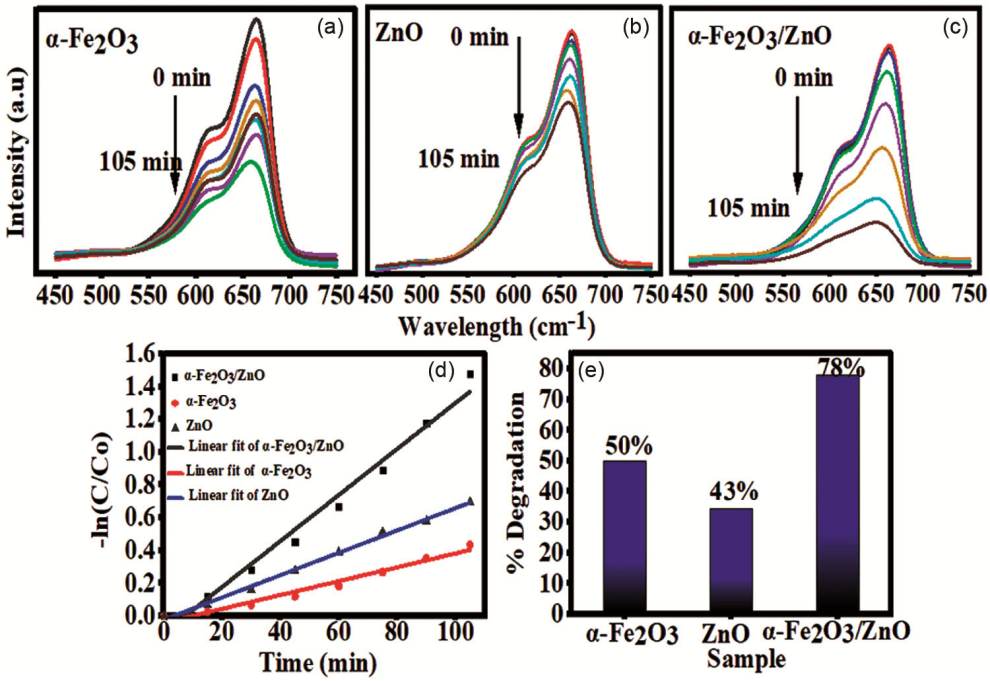

Fig. 4 — Absorption spectra of dye (a) pure α–Fe_2O_3 (b) pure ZnO and (c) α–Fe_2O_3/ZnO nanocomposite at different time intervals, (d) % degradation of synthesized samples (e) linearly fitted curves of –ln(C/Co) versus exposure time of pure α–Fe_2O_3, ZnO and α–Fe_2O_3/ ZnO nanocomposite.

ZnO. For pure α-Fe_2O_3, absorption peak at 1548 cm^{-1} is due to –OH bending and peak at 1648 $cm^{-1}$is attributed to the formation of carbonate species. The peak at 1351 cm^{-1} and 918–700 cm^{-1}[7] represents C-N vibration and Fe–O stretching. The peaks at 2340 cm^{-1} and 1709 cm^{-1} are attributed to C–H stretching and C–O stretching respectively. For pure ZnO, the region between 400 and 600 cm^{-1} is due to Zn–O as shown in Fig. 3. Peak at 1598 cm^{-1} is due to H–O–H bending vibration. The band at 2350 cm^{-1} stands for carbonate that comes from atmospheric carbon dioxide[8]. The band at 1631 cm^{-1}(bending) is due to the asymmetrical stretching of zinc carboxylate. The peaks at 1371 cm^{-1} and 643 cm^{-1} result in C-O absorption of ZnO surface and representing amines (N–H). The weak Zn–O stretching frequencies are also observed at 881 cm^{-1}[10]. In α–Fe_2O_3/ZnO nanocomposite, all the peaks of pure α–Fe_2O_3 and pure ZnO are observed showing the successful formation of nanocomposite.

3.4. Photocatalytic activity

Prepared samples were investigated for their photocatalytic activity towards methylene blue (MB) dye using ultraviolet (UV) light. The degradation rate of MB dye is indicated by a decrease in absorption peak intensity from 0 min to 105 min shown in Fig. 4(a-c). Equilibrium adsorption is achieved after 30 min stirring in dark. Poor photodegradation activity is shown by pure ZnO and pure α–Fe_2O_3 nanoparticles as compared to α–Fe_2O_3/ZnO nanocomposite because nanocomposite inhibited the high recombination time of charge carriers. Degradation percentage given by,

$$(1 - C/C_0) \times 100\%$$

Here, C_0 is the initial concentration after equilibrium adsorption and C is the remaining concentration of MB. The synthesized nanocomposite exhibits 78% degradation rate in 105 min as depicted in Fig. 4(d). UV irradiation results to excite the electrons moving from the valence band to conduction band leaving behind holes. Electrons interacting with oxygen molecules result in the formation of highly reactive superoxide anions, and holes in the valence band interacting with the hydroxyl group produce highly reactive hydroxyl radicals which are responsible for degradation performance. The first-order kinetics of photocatalytic degradation is followed bya linear plot between $-\ln(C/C_o)$

and time shown in Fig. 4(e). By linearly fitting the curve between $-\ln(C/C_o)$ and time, rate constant (k) can be determined.

4 Conclusion

Pure α–Fe_2O_3, pure ZnO, and α–Fe_2O_3/ZnO nanocomposite has been prepared by hydrothermal technique for investigating the structural and optical behaviour in wastewater treatment. According to XRD results, samples were as-prepared with an average crystallite size of 29.10 nm, 15.45 nm, and 11.77 nm. The optical band gap evaluated from Tauc's plot was found to be 2.50 eV for α–Fe_2O_3/ZnO nanocomposite. Photodegradation efficiency for MB dye was found to be 78% by α–Fe_2O_3/ZnO nanocomposite. The as-synthesized nanocomposite could be appropriate for wastewater treatment.

References

1 Kumari H, Sonia, Suman, Ranga R, Chahal S, Devi S, Sharma S, Kumar S, Kumar P, Kumar S, Kumar A & Parmar R, *Water Air Soil Pollut*, 234 (2023) 349.

2 Sonia, Kumari H, Suman, Chahal S, Devi S, Kumar S, Kumar P & Kumar A, *Appl Phys A: Mater Sci Process*, 129 (2023) 91.

3 Devi S, Chahal S, Singh S, Kumar P, Kumar S, Kumar A & Kumar V, *Ceram Int*, 49 (2023) 20071.

4 Liu J, Yang S, Wu W, Tian Q, Cui S, Dai Z, Ren F, Xiao X & Jiang C, *ACS Sustain Chem Eng*, 3 (2015) 2975.

5 Yan W, Fan H & Yang C, *Mater Lett*, 65 (2011) 1595.

6 Navale S T, Khuspe G D, Chougule M A, Patil V B, *Org Electron*, 15 (2014) 2159.

7 Suman, Singh S, Kumar A, Kataria N, Kumar S & Kumar P, *J Environ Chem Eng*, 9 (2021) 106266.

8 Kumar P, Pal J S, Kumar Y, Kumar Y, Gaur A, Malik H K, Asokan K, *Curr Appl Phys*, 12 (2012) 1166.

9 Sadollahkhani A, Kazeminezhad I, Lu J, Nur O & Hultman L, *RSC Adv*, 4 (2014) 36940.

10 Muthukumaran S & Gopalakrishnan R, *Opt Mater*, 34 (2012) 1946.